Supporting Information

Damping of Acoustic Vibrations of Immobilized Single Gold Nanorods in Different Environments

Kuai Yu[1,2], Peter Zijlstra[1,3], John E. Sader[4,5], Qing-Hua Xu[2], Michel Orrit[1]

[1]Institute of Physics, Leiden University, Leiden, The Netherlands

[2]Department of Chemistry, and NUS Graduate School for Integrative Sciences and Engineering, National University of Singapore, Singapore

[3]Department of Applied Physics, Eindhoven University of Technology, Eindhoven, The Netherlands

[4]Department of Mathematics and Statistics, The University of Melbourne, Victoria, 3010, Australia

[5]Kavli Nanoscience Institute and Department of Physics, California Institute of Technology, Pasadena, California 91125, USA

Particle temperature after pump and probe excitation:

Here we estimate the particle lattice temperature increase due to the pump and probe lasers pulses. The energy E_{abs} absorbed by the nanoparticle from pulses with energy E_{pulse} can be approximated as $E_{abs}=\sigma_{abs}/A\times E_{pulse}$, where σ_{abs} is the absorption cross-section of the nanoparticle at the wavelength of the pump or probe laser and A is the cross-sectional area of the laser beam in the focal plane. The value for A was obtained from the spot size in raster scans at zero time delay, and we found $A=1.52\times10^{-13}$ m^2. The absorption cross-section of a nanorod, σ_{abs}, was estimated for an ellipsoid in the electrostatic approximation.[1] For a typical particle of 25 nm × 54 nm in air and water, the calculated absorption spectra are shown in Figure S1 using the effective refractive index to match the calculated plasmon wavelength to the measured spectra as shown in Figure 1c. For example, the calculated absorption cross section values at 785 nm are 1.45×10^{-16} m^2 and 3.75×10^{-16} m^2 in air and water, respectively, as shown in Table S1.

The initial temperature increase of the lattice can then be calculated from the absorbed energy as $\Delta T=E_{abs}/C_pV_p$, where C_p is the heat capacity of bulk solid gold (24.9×10^5 JK^{-1}m^{-3}) and V_p is the gold nanorod volume (2.24×10^{-23} m^3). For the typical pump and probe pulse energies and wavelengths used, we find upper limits of the transient lattice temperature of about 600 K at zero probe delay. Note that the temperature rise due to the probe laser is evaluated for a wavelength on the peak of the plasmon.

For the nanorod in water, the lattice temperature decays on a time scale of around 100 ps, about 100 times shorter than the pulses separation (~ 13 ns). Due to this low duty cycle the time-averaged temperature increase of the nanorod is <10 K, and hence no reshaping is expected. This is in agreement with ultrafast studies on ensembles of gold nanorods, where no structural reshaping was observed for transient lattice temperatures below 1000 K.[2] More importantly, structural reshaping can be verified by recording white-light spectra before and after the pump-probe measurements. Under the excitation conditions employed in this report, all the particles are stable.

Table S1. Calculated upper bounds for the lattice temperature increase after the simultaneous absorption of pump and probe pulses for 25 nm × 54 nm nanorod in air and water. Note that the probe wavelength is taken on the plasmon peak.

Nanorod	Pulses	σ $(m^2)@\lambda_{pulse}$	E_{pulse} (pJ)	E_{abs} (fJ)	ΔT_{max} (K)
Air	Pump (λ= 785nm)	1.45×10^{-16}	10	9.5	170
	Probe (λ= 603nm)	9.41×10^{-15}	0.2	12.4	220
Water	Pump (λ= 785nm)	3.75×10^{-16}	5	12.3	220
	Probe (λ= 650nm)	1.64×10^{-14}	0.2	21.6	390

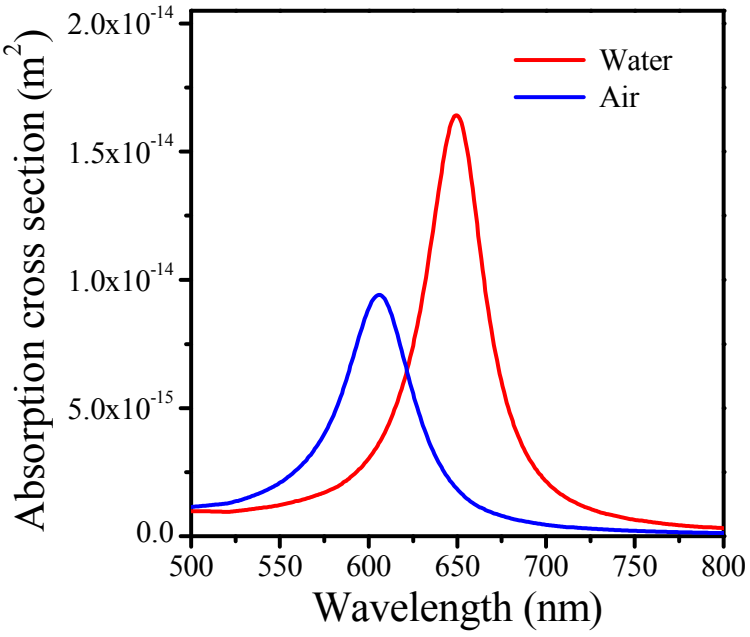

Figure S1. Calculated absorption cross section of a 25 nm × 54 nm prolate spheroid immersed in air and water. To account for the presence of the substrate we used an effective medium refractive index, which was chosen such that the calculated plasmon wavelength matches the measured values shown in Fig. 1c in the main text (n=1.3 for the particle in air, n=1.5 for the particle in water).

Red-shift of the plasmon resonance by a thin film of water:

Mie theory gives an exact solution for the absorption and scattering cross sections, but applies only to spherical particles. The theoretical description of scattering of light by nanorods of finite length is complicated due to the lack of symmetry in the problem. To be able to deal with more general particle shapes, we will therefore approximate the shape of a nanorod with a very small ellipsoid, for which a simple solution to the scattering problem was developed in 1912 by Gans.[3]

The theory developed by Gans can also be used to calculate the absorption cross section of a confocal core-shell spheroid. This allows us to approximate the effect of the thin water layer by modeling it as a water shell surrounding the spheroid. The inner or core spheroid has semiaxes a_1, b_1, c_1; The outer spheroid has semiaxes a_2, b_2, c_2. The polarizability in a field parallel to major axis can then be expressed as:[1]

$$\alpha_3 = \frac{V((\varepsilon_2 - \varepsilon_m)[\varepsilon_2 + (\varepsilon_1 - \varepsilon_2)(L_3^{(1)} - fL_3^{(2)})] + f\varepsilon_2(\varepsilon_1 - \varepsilon_2))}{([\varepsilon_2 + (\varepsilon_1 - \varepsilon_2)(L_3^{(1)} - fL_3^{(2)})][\varepsilon_m + (\varepsilon_2 - \varepsilon_m)L_3^{(2)}] + fL_3^{(2)}\varepsilon_2(\varepsilon_1 - \varepsilon_2))}$$

where $V = 4\pi a_2 b_2 c_2 / 3$ is the volume of the particle, $f = a_1 b_1 c_1 / a_2 b_2 c_2$ is the fraction of the total particle volume occupied by the inner ellipsoid, and $L_3^{(1)}$ and $L_3^{(2)}$ are the geometrical factors for the major axis of the inner and outer ellipsoids. The calculated plasmon shift of the core-shell spheroid as a function of the thickness of water shell is shown in Figure S2.

In our experiments, the plasmon resonance of a gold nanorod red-shifts by ~50 nm when the surrounding medium is changed from air to water. After evacuation of the flow cell the red-shift reduces to ~30 nm, indicating that a thin layer of water remains on the particle. This plasmon shift can thus be used as an indicator for changes in the thickness of the water film surrounding the particle. Although the exact geometry of the water layer on the particle in our experiments is not known, this simplified model indicates that the effective thickness of the layer is in the range of a few to tens of nanometers.

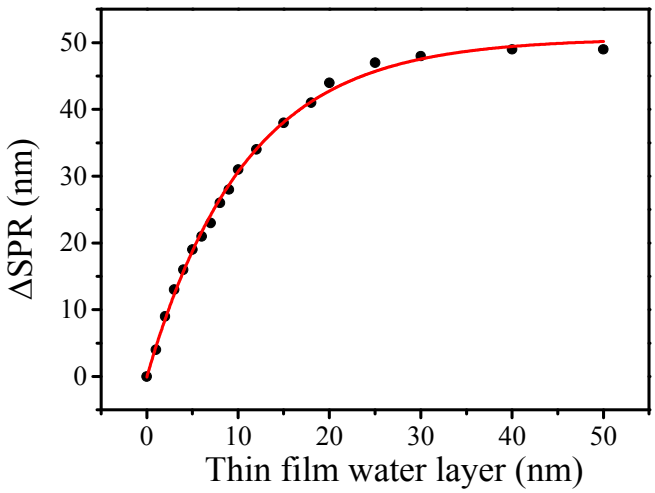

Figure S2. Calculated longitudinal surface plasmon resonance shift of a 25 nm × 54 nm core-shell spheroid in air for different water shell thicknesses. The dielectric function of bulk gold is used as reported by Johnson and Christie.[4] The red line is a guide to the eye.

Acoustic vibrations of single gold nanorods under a thin film of water:

For all pump-probe spectra measurements shown here, we have recorded the white-light spectra to determine the plasmon shift, and also to help to choose the proper probe wavelength to get optimum contrast of the vibrations in the time traces.

In Figure S3 we show the delay traces of a single gold nanorod in a thin film of water. Red lines are fits to the experimental data using eq 1 in the main text, from which we obtain the quality factor of the vibration. The water was gradually evaporated with a gentle flow of dry nitrogen, indicated by a gradual blue-shift of the plasmon resonance. After some time the nitrogen flow was stopped, and we recorded a vibration trace of the particle. We checked the plasmon resonance before and after the pump-probe measurements and found no detectable shift, indicating that the water film is stable on the timescale of our measurement.

Figure S4 shows the quality factor of the breathing and extension modes for different plasmon shifts (i.e. different water film thicknesses) and different particles. For all particles the quality factors of the breathing and extension modes decrease for increasing water-film thickness. Also note that the cooling time of the particle increases from the top to the bottom trace, caused by the reduction of the amount of water on the particle.

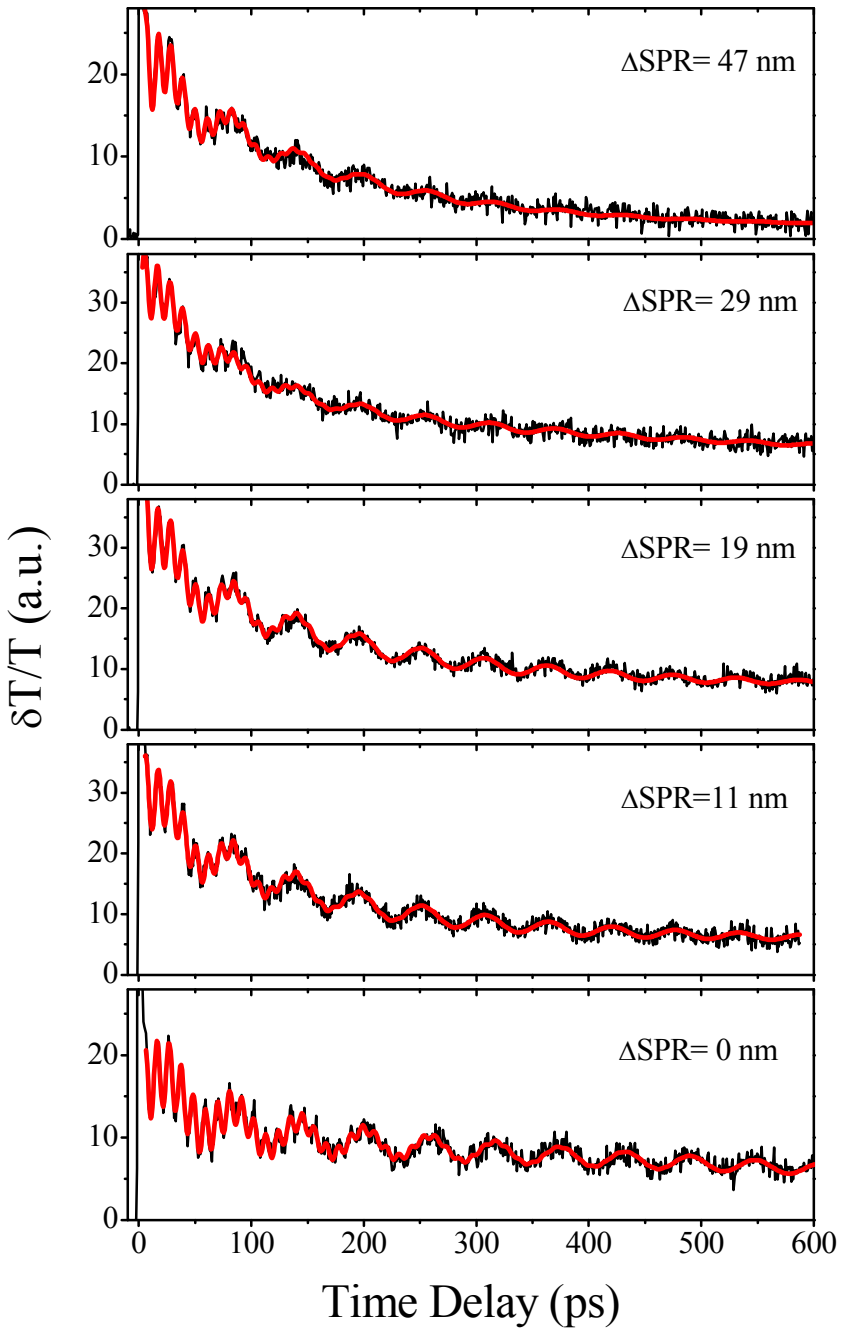

Figure S3. Acoustic vibrations of a single gold nanorod in different water environments as indicated by the longitudinal plasmon resonance shift. The particle is fully immersed in water for the top trace ($\Delta SPR = 47$ nm) and the water was gradually evaporated until no further blue-shift was observed (bottom trace, $\Delta SPR = 0$ nm). The red lines are fits using eq 1 in the main text.

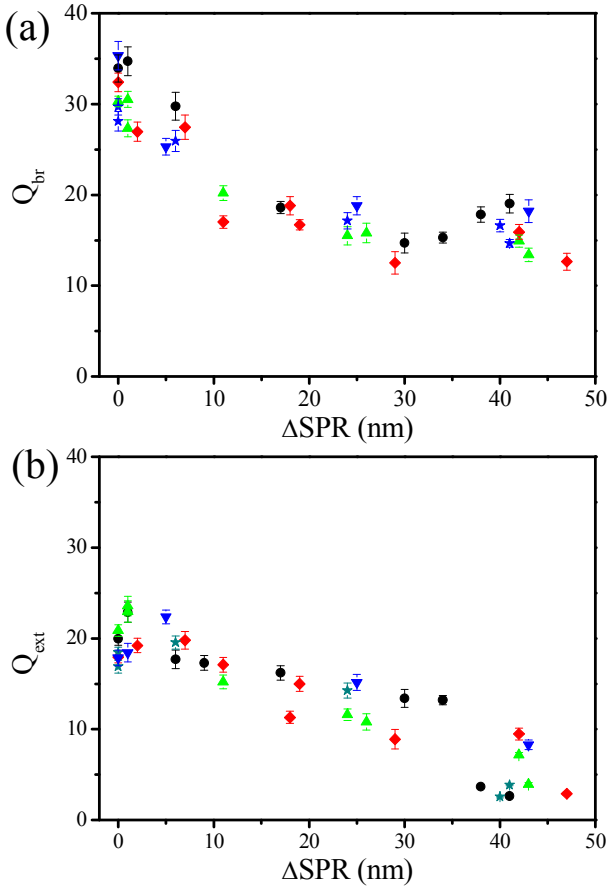

Figure S4. Quality factors for (a) the breathing mode and (b) the extension mode as functions of plasmon red-shift (compared to the plasmon for a particle on a substrate in air). The different symbols indicate different particles.

Repeated changes of the environment between water and air:

We verified the reproducibility of the measurements by repeatedly measuring the vibration traces of the same particles in water and in air. After immersion in water the liquid was evacuated from the flow cell and remaining water was evaporated by a gentle flow of nitrogen. Complete evaporation of the water was verified by the blue-shift of the plasmon wavelength, which was the same for all the measurements conducted in the respective medium.

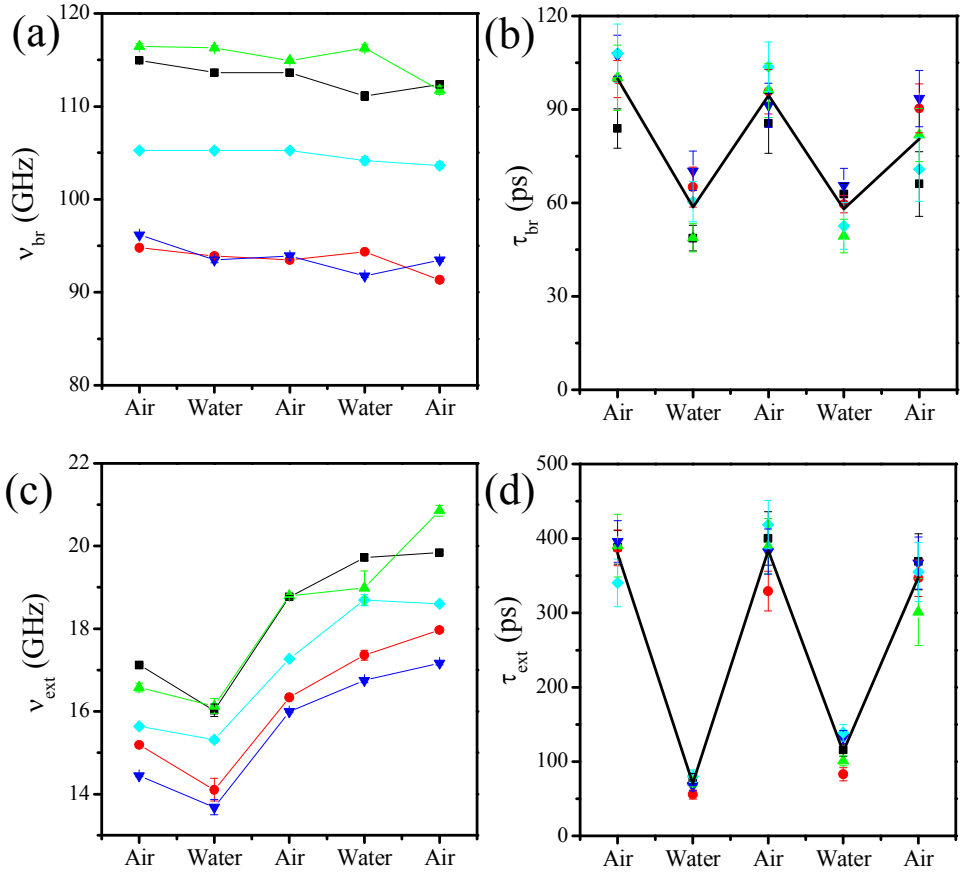

Figure S5. Vibration frequency and damping time of gold nanorods after repeated changes of the local environment. (a) Vibration frequencies, (b) damping times of the breathing mode, (c) vibration frequencies and (d) damping times of the extension mode of five different gold nanorods as indicated by different colors.

Vibrations of an embedded spherical particle:

To estimate the effect of the environment on the breathing mode of the nanorods we approximated our short aspect-ratio particles as spheres. For spherical particles only the radially symmetric breathing mode is excited. The radius of the sphere was chosen such that its breathing frequency is the same as the breathing frequency of our nanorods. Firstly, we calculate the damping due to the impedance mismatch of the gold with its environment. The frequencies and damping times of the breathing mode of an elastic gold sphere embedded in an elastic medium can be calculated according to the complex frequency model.[5] The frequencies ω_n and damping rate γ_n of a sphere are given by:

$$\omega_n + i\gamma_n = \xi_n c_l^{(s)} / R$$

where $c_l^{(s)}$ is the longitudinal speed of sound in bulk gold, and R is the radius of the sphere. The complex eigenvalue ξ_n can be calculated from the following equation:

$$\xi \cot(\xi) + \frac{\xi^2(1+i\xi/\alpha)}{\eta\xi^2 - 4\alpha^2\gamma^2(1-1/\eta\beta^2)(1+i\xi/\alpha)} = 1,$$

where the different parameters are defined by:

$$\alpha = c_l^{(m)} / c_l^{(s)}, \qquad \beta = c_t^{(m)} / c_t^{(s)}, \qquad \gamma = c_t^{(m)} / c_l^{(m)}, \qquad \eta = \rho^{(m)} / \rho^{(s)},$$

Where $c_{l,t}^{(m),(s)}$, and $\rho^{(m),(s)}$ are the longitudinal or transverse sound velocity and the density of the matrix (m) and particle (s) materials. Then the angular mode frequency $\omega_n = \mathrm{Re}(\xi_n)\, c_l^{(s)} / R$ and damping rate $\gamma_n = \mathrm{Im}(\xi_n)\, c_l^{(s)} / R$ can be calculated. We estimate the quality factor by considering a gold nanosphere with a diameter of 32 nm (which has the same breathing frequency as the gold nanorods), yielding $Q_{imp} = 52.9 \pm 0.5$ in water.

Secondly, we estimate the effect of viscous damping following the approach by Saviot et al.,[6] which we previously used to analyze results for single Au nanoparticles optically trapped in water.[7] In the calculation of the viscous damping we have used the viscosity of water at 30 ^{o}C as in Saviot et al.[6] The model includes sound radiation and damping by bulk and shear viscosities by writing the speeds of sound in the environment as $c_l^{(env)} = ((\lambda_L + 2\mu_L + i\omega(\lambda + 2\mu)) / \rho_{H_2O})^{1/2}$ and $c_t^{(env)} = ((\mu_L + i\omega\mu) / \rho_{H_2O})^{1/2}$, where μ_L and λ_L are Lamé constants, and μ and λ are the shear and bulk viscosity coefficients. We find a minor correction to Q_{imp}, yielding $Q_{imp+visc} = 49.5 \pm 0.5$ for the overall quality factor. The effect of viscosity on the damping of the breathing mode of the nanoparticle is thus small.

Table S2: Longitudinal and transverse speed of sound, density of water, air and gold at room temperature. Standard deviations in the calculated values are also included by considering the particle size distribution of the gold nanorods with an ensemble average size of 25 ± 3 nm in width and 54 ± 3 nm in length determined by TEM measurements.

Material	c_l (m.s^{-1})	c_t (m.s^{-1})	ρ (kg.m^{-3})
Water	1480	0	998
Air	343	-	1.18
Gold	3240	1200	19300

Fluid damping of the extensional mode of a gold nanorod:

1. Unbounded fluid

A general asymptotic theory for a slender rod immersed in an unbounded viscous fluid was presented in Ref. [10]. Here, we apply this theory to estimate the quality factor due to the surrounding fluid.

The extensional mode resonant frequencies in a vacuum of an axisymmetric cylindrical rod are given by[8]

$$\omega_{vac} = \frac{2n+1}{L}\pi\sqrt{\frac{E}{\rho^{(s)}}},$$

where $n = 0,1,2,...$ is the mode number, E is the Young's modulus along the long axis of the rod, $\rho^{(s)}$ is the density of bulk gold, and L is the rod length.

The surrounding fluid modifies the resonant frequency and gives rise to finite damping. The theory in Ref. [10] specifies the following results for the fundamental ($n = 0$) extensional mode. The fundamental angular resonant frequency, ω_R, and quality factor in fluid Q_{fluid} are:

$$\omega_R = \omega_{vac}[1+\Gamma_{cyl}(\omega_R)]^{-1/2},$$

$$Q_{fluid} = 1+\frac{1}{\Gamma_{cyl}(\omega_R)}$$

where

$$\Gamma_{cyl}(\omega) = \frac{1}{\rho^{(s)}}\sqrt{\frac{2\mu\rho^{fluid}}{\omega R^2}}.$$

Here, μ is the fluid shear viscosity, ρ^{fluid} the fluid density, and R is the radius of the rod. This predicts that the quality factor varies in proportion to $(\mu\rho^{fluid})^{1/2}$.

For gold nanorods with an ensemble average size of 25 ± 3 nm in width and 54 ± 3nm in length immersed in water, the above formula gives a quality factor due to the fluid of $Q_{fluid} = 53.8 \pm 5.7$. An intrinsic quality factor $Q_{intr} = 22$ was chosen to match experimental data in air; this intrinsic value is consistent with previous measurements.[9-10]

2. Particle near a surface

We now estimate the quality factor when the particle is in close proximity to a surface and surrounded by fluid; this is the experimental situation of this study. As discussed, the precise geometry of the particle/water system is not known. A simplified analysis that models this effect is therefore presented. We consider an oscillating cylinder encased by a coaxial stationary cylinder (of larger radius), with fluid confined between the cylinders. Setting the radius of the stationary cylinder to infinity recovers the unbounded solution of Ref. [10].

As in Ref. [10], the viscous boundary layer thickness surrounding the oscillating cylindrical particle is assumed to be small, relative to the particle radius, *R*. Since we are interested in the case of close proximity to the surface, the separation *h* between the oscillating and stationary cylinders is also considered to be much smaller than the cylinder radius. Thus, the hydrodynamic load at each surface element of the oscillating cylinder is given by that of oscillatory Couette flow between one oscillating and one stationary planar wall, separated by a distance *h*.

Under this modification, the analysis of Ref. [10] then gives the complex eigenfrequency, ω_R, for this problem

$$\omega_R = \omega_{vac}\left(1+\Gamma_{surf}(\omega_R)\right)^{-1/2},$$

where

$$\Gamma_{surf}(\omega) = \frac{\rho^{fluid}}{\rho^{(s)}}\frac{1+i}{\sqrt{\beta}}\frac{1}{\tanh\left(\frac{h}{R}[1-i]\sqrt{\beta}\right)},$$

$$\beta = \frac{\rho^{fluid}\omega R^2}{\mu}.$$

and *i* is the usual imaginary unit. Note that as the separation *h* is increased, we recover the result reported in Ref. [10] for an unbounded fluid, as required.

To proceed, we evaluate the real and imaginary components of the complex eigenfrequency, ω_R, in the asymptotic limit of small h/R. This gives the leading order results:

$$\omega_r = \omega_{vac},$$

$$\omega_i = -\frac{\mu}{2hR\rho^{(s)}},$$

where ω_r and ω_i refer to the real and imaginary components of the complex eigenfrequency, ω_R. The quality factor is then obtained from $Q = -\omega_{vac}/(2\omega_i)$, where the resonant frequency in fluid has been approximated by its value in vacuum. This yields the required result

$$Q = \frac{\rho^{(s)}\omega_{vac}hR}{\mu}.$$

This formula is valid provided the separation *h* is much smaller than the viscous penetration depth, i.e., $h << R/\sqrt{\beta}$, which is the case in the present measurement.

References

(1) Bohren, C. F.; Huffman, D. R. Absorption and Scattering of Light by Small Particles. *John Wiley & Sons, New York.* **1982**.

(2) Zijlstra, P.; Chon, J. W. M.; Gu, M. White Light Scattering Spectroscopy and Electron Microscopy of Laser Induced Melting in Single Gold Nanorods. *Phys. Chem. Chem. Phys.* **2009**, *11*, 5915.

(3) Gans, R. ber Die Form Ultramikroskopischer Goldteilchen. *Ann. Phys.* **1912**, *342*, 881.

(4) Johnson, P. B.; Christy, R. W. Optical Constants of Noble Metals. *Phys. Rev. B* **1972**, *6*, 4370.

(5) Voisin, C.; Christofilos, D.; Del Fatti, N.; Vallée, F. Environment Effect on the Acoustic Vibration of Metal Nanoparticles. *Physica B* **2002**, *316–317*, 89.

(6) Saviot, L.; Netting, C. H.; Murray, D. B. Damping by Bulk and Shear Viscosity of Confined Acoustic Phonons for Nanostructures in Aqueous Solution. *J. Phys. Chem. B* **2007**, *111*, 7457.

(7) Ruijgrok, P. V.; Zijlstra, P.; Tchebotareva, A. L.; Orrit, M. Damping of Acoustic Vibrations of Single Gold Nanoparticles Optically Trapped in Water. *Nano Lett.* **2012**, *12*, 1063.

(8) Hu, M.; Wang, X.; Hartland, G. V.; Mulvaney, P.; Perez-Juste, J.; Sader, J. E. Vibrational Response of Nanorods to Ultrafast Laser Induced Heating: Theoretical and Experimental Analysis. *J. Am. Chem. Soc.* **2003**, *125*, 14925.

(9) Zijlstra, P.; Tchebotareva, A. L.; Chon, J. W. M.; Gu, M.; Orrit, M. Acoustic Oscillations and Elastic Moduli of Single Gold Nanorods. *Nano Lett.* **2008**, *8*, 3493.

(10) Pelton, M.; Wang, Y.; Gosztola, D.; Sader, J. E. Mechanical Damping of Longitudinal Acoustic Oscillations of Metal Nanoparticles in Solution. *J. Phys. Chem. C* **2011**, *115*, 23732.